J Mater Sci (2008) 43:645–651
DOI 10.1007/s10853-007-2149-x

Effect of deposition pressure on the adhesion and tribological properties of a-CN_xH films prepared by DC-RF-PECVD

Jun Ding · Junying Hao · Qunji Xue · Weimin Liu

Received: 4 January 2007 / Accepted: 7 September 2007 / Published online: 17 October 2007
© Springer Science+Business Media, LLC 2007

Abstract Hydrogenated carbon nitride (a-CN_xH films) was deposited on *n*-type single-crystal Si (100) by direct current radio frequency plasma-enhanced chemical vapor deposition (DC-RF-PECVD), under the working pressure of 5.0–17.0 Pa, using the CH_4 and N_2 as feedstock. The composition and surface morphology of the a-CN_xH films were characterized by means of Raman spectroscopy and atomic force microscopy, while the Young's modulus, elastic recovery, adhesion strength, and tribological properties were evaluated using nano-indentation, scratch test and friction test system. It was found that the surface roughness and Raman spectra peak intensity ratio I_D/I_G of the films increased with the increase of working pressure, while the Young's modulus, elastic recovery and adhesion strength of the films significantly decreased. Moreover, the tribological properties of the films also varied with the working pressure. The wear life sharply increased with the increase of working pressure from 5.0 Pa to 7.5 Pa, further, an increase in the deposition pressure led to a gradual decrease in the wear life, consequently, the a-CN_xH film deposited at 7.5 Pa exhibited the longest wear life. The deposition pressure seemed to have slight effect on the average friction coefficients, whereas the surface roughness and adhesion strength have deteriorated with increasing deposition pressure.

J. Ding · J. Hao (✉) · Q. Xue · W. Liu
State Key Laboratory of Solid Lubrication, Lanzhou Institute of Chemical Physics, Chinese Academy of Sciences, Lanzhou 730000, P.R. China
e-mail: jyhao33@yahoo.com.cn

J. Ding
Graduate School, Chinese Academy of Sciences, Beijing 100039, P.R. China

Introduction

Recently, there has been tremendous interest in the investigation of carbon nitride (CN_x) films, because Liu and Cohen theoretically predicted that the β-C_3N_4 phase would be harder than diamond [1–3]. Although it is very difficult to fabricate the predicted crystalline phase in the deposition process, a-CN:H films still exhibit many attractive properties, such as high wear resistance, low friction coefficient, and good chemical inertness, which stimulate people to make more efforts to synthesize various carbon nitride films and many approaches are employed including reactive sputtering [4–7], ion beam deposition [8–11], pulsed laser deposition [12, 13], plasma-enhanced chemical vapor deposition (PECVD) [14–16]. The deposition parameters such as the total pressure and gas ratio are crucial to the properties and microstructure of the films, and the effect of deposition pressure on the composition and structure of a-CN_xH films has been studied extensively [14, 17, 18]. However, few studies are related to the elastic parameter, adhesion, and tribological properties of the films, which are very important to practical applications [18]; additionally, the role of nitrogen during the film growth is not yet clear, which demands more light to be shed on the study of a-CN_xH films on the mechanical and tribological characteristics so as to acquire more insight into the properties changes of the a-CN_xH films with the working pressure.

Accordingly, a series of a-CN_xH films were prepared using of DC-RF-PECVD, which had the flexibility to qualitatively control the ion current density and ion kinetic energy by adjusting the ion current and DC current, respectively [19, 20]. The investigation of the composition and microstructure of the a-CN_xH films were reported in our previous work [21]. Therefore, in this article, the study is mainly focused on the elastic parameter, adhesion

strength, and the friction and wear behaviors of the films produced at different working pressure.

Experimental details

The a-CN_xH films were deposited on the *n*-type single-crystal Si (100) wafers by a DC-RF-PECVD system at working pressure varying from 5.0 Pa to 17.0 Pa. The film deposition process has been introduced in Ref. [21]. The thickness of the films was controlled at about 500 nm and the experimental parameters are summarized in Table 1.

An SPM-9500 atomic force microscope (AFM) operating with a Si_3N_4 probe in a “contact force” mode was used to observe the surface morphologies and to determine the surface roughness of the films. A triple Raman spectroscope (Jobin Yvon T64000) working with Ar laser beam of 514.5 nm was used as the excitation source to determine the chemical structure of the films.

The mechanical properties of the films have been evaluated using a Nano Indenter™ II microprobe. The information of the nano-indenter was elsewhere introduced [21, 22]. The maximum indentation depth was kept at 50 nm in each film, so as to minimize the substrate effect. The respective load and displacement curves were continuously recorded during both the loading and unloading courses. Five replicate indentations were made for each film sample. The Young’s modulus, the penetration displacement of the indenter at maximum load h_{max}, the displacement of the residual indent h_{res}, and the elastic recovery have been used to characterize the elastic properties of the films.

The adhesion strengths of the films were evaluated on a WS-92 scratch test system (Lanzhou Institute of Chemical Physics, Lanzhou, China). A three-sided pyramidal Berkovich indenter diamond tip was driven to scratch the a-CN_xH films surfaces at a load rate of 25 N/min, the end load of 60 N, and the trace length in 4.0 mm. The morphologies of the scratched tracks of the films were observed on a JSM-5600LV scanning electron microscope (SEM).

Table 1 Summary of the deposition conditions for the a-CN_xH films

Item	Parameter
CH_4 gas flow rate (sccm)	20.0
N_2 gas flow rate (sccm)	20.0
RF power (W)	100
DC bias (V)	200
Deposition pressure (Pa)	5.0, 7.5, 10.0, 15.0, 17.0
Film thickness (nm)	500

The wear behaviors of the films were evaluated on an UMT-2MT test system (Center for Tribology, Inc., California, USA) in reciprocal-sliding mode. The a-CN_xH films on the silicon substrates were made to slide against a Si_3N_4 ceramic ball (diameter 3 mm, hardness HV1500-1,700 Kgm^{-2}) at a sliding velocity of 60 mm/s and a load of 1.0 N. All the ceramic balls were cleaned ultrasonically in an acetone bath prior to measurement and a new ball or a new position of the ball was used for each run of the wear testing. All the scratch test and friction tests were conducted at a room temperature about 20–26 °C and relative humidity of 40–45%. The friction coefficient and sliding time were automatically recorded during the test.

Results and discussion

Characterization of films

Raman spectroscopy is popularly used to probe the quality of carbon films due to its ability to distinguish between different bonding types and domain sizes [23, 24]. Usually, the Raman spectra of the a-CN_xH films are characterized by a graphitic band (G-band) around 1,559 cm^{-1} and disordered band (D-band) around 1,372 cm^{-1} in the spectral region within 1,200–1,800 cm^{-1}. The details for the G- and D-peaks of a-CN_xH films are reported elsewhere [25].

Figure 1 shows the Raman spectra of the a-CN_xH films deposited at different total working pressures, which were deconvoluted into two Gaussian peaks. It is seen that the Raman spectra of the films were closely dependent on the working pressure. For the film deposited at 5.0 Pa, a G peak around 1,534 cm^{-1} and a weak D shoulder around 1,368 cm^{-1} were observed. The obvious shift of two peaks

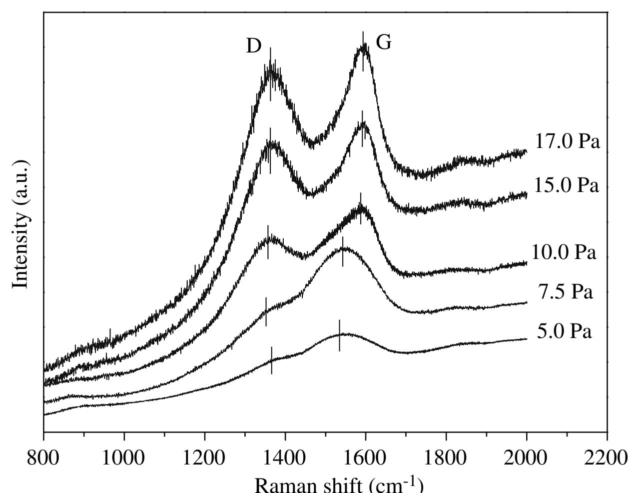

Fig. 1 Raman spectra of the a-CN_xH films deposited at various working pressures

position toward higher wave number was found with the increase of pressure. Namely, as the pressure is raised from 5.0 Pa to 17.0 Pa, the G peak position shifts toward higher wave number from 1,534 cm^{-1} to 1,364 cm^{-1}, and the D peak position also shifts upward from 1,368 cm^{-1} to 1,392 cm^{-1}. This position shift of the peaks is supported by a change in the I_D/I_G ratio and a decrease of G linewidth. This indicates a change of the size of sp^2 C domains at very-low nitrogen content in the films [26, 27]. Namely, these shifts in the G and D peaks position corresponded to a decrease of the sp^3 content in the deposited films. In other words, the increase of the pressure referred to an increase in the graphite-like domains of the a-CN_xH films, which conformed well to the corresponding AFM analysis latter on. Moreover, the increase of the I_D was observed clearly with increasing pressure, which leads to the increase of the I_D/I_G from 0.85 to 1.87. It seems that the pressure increased the ratio between the spring constant of bonds and average mass of the atoms in the carbon films [27]. The increase of the I_D also accounted for the fact that the increase of N content results in the structural transformation from sp^3 to sp^2-like carbon–nitrogen network in the a-CN_xH films. This result was in good agreement to that of the relevant N/C atomic ratio analysis [21].

The surface morphology of the films is important for tribological applications. The representative three-dimensional AFM images shown in Fig. 2, illustrates the effect of the total working pressure on the roughness of the a-CN_xH films. Based on Fig. 2, the surface roughness, root-mean-square (rms), of the films prepared at different deposition pressures are listed in Table 2. It was seen that the a-CN_xH films deposited at lower working pressure were composed of small and compact grains with a dimension within 3–20 nm. The film surfaces are uniform and smooth, and the roughness was about 0.20 nm, which was almost as same as that of the original silicon wafer surface. However, the film roughness increased with increasing deposition pressure. Namely, the films prepared at 5.0 or 10.0 Pa and 17.0 Pa had the roughness of 0.18 or 0.22 nm, but a roughness of 0.5 nm was obtained for the films prepared at 17.0 Pa, and the surface of the deposited film prepared at high pressure showed the larger grains and obvious defect. On one hand, most of the CH_4 and N_2 molecules in the deposition chamber were decomposed into neutral radicals and atomic or ionic species at low working pressure and deposited in the growing film as the small cluster size. On the other hand, it was more difficult for the CH_4 and N_2 molecules to be completely decomposed at a high working pressure at a fixed RF power, and fractional CH_4 and N_2 entered the deposited films in molecules modes, subsequently the cluster size increased to certain extent. Moreover, the increase in the surface roughness of the a-CN_xH films with increasing working pressure could also related to the recombination of N_2. The recombination

Table 2 Summary of the scratch, friction and wear test data for a-CN_xH films

Item	Properties				
Working pressure (Pa)	5.0	7.5	10.0	15.0	17.0
Surface roughness (nm)	0.18	0.19	0.22	0.34	0.50
Elastic recovery (%)	82	80	78	74	71
Critical load (N)	52.0	45.0	42.0	34.0	30.0
Friction coefficient (μ)	0.19	0.20	0.19	0.19	0.18

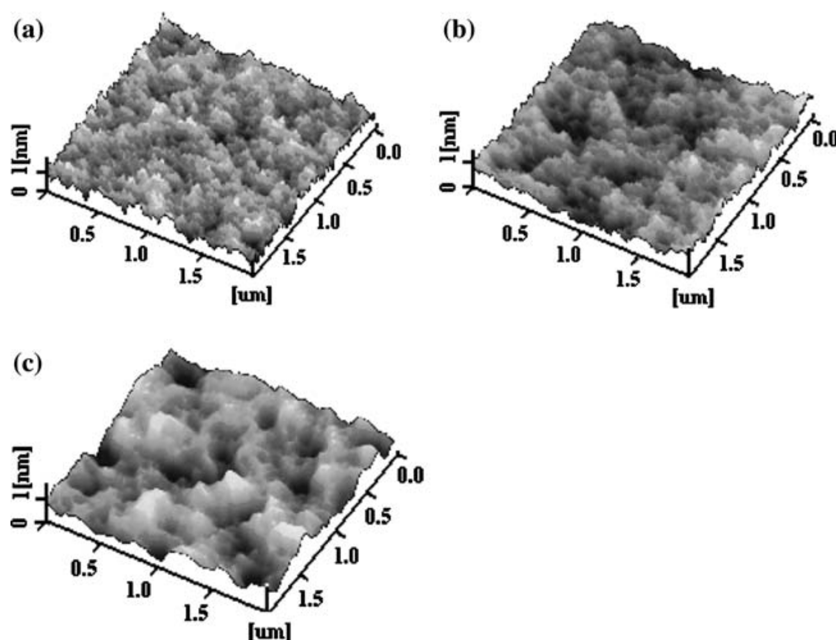

Fig. 2 AFM images of the a-CN_xH films prepared at a working pressure of (**a**) 5.0 Pa, (**b**) 10.0 Pa, and (**c**) 17.0 Pa

between the active nitrogen ions in the plasma and the substrate surface led to a change in the surface mobility. Consequently, the graphite-like surface structure was formed inside the a-CN_xH film and the surface roughness of the film increased to certain extent. Besides, the increase of the roughness of films also might be attributed to the increased number of sp^2 bonded carbon sides [28].

Elasticity of films

Figure 3 shows the representative load-displacement curves of the a-CN_xH film deposited at working pressure of 5.0 Pa. The hardness (H) has been reported in Ref. [21]. The reduced modulus (E_r) of the a-CN_xH films were obtained from load–unloading curves. The Young's modulus of the deposited films was calculated using following equation:

$$1/E_r = (1 - v_s^2)/E_s + (1 - v_i^2)/E_i$$

where E_r is the reduced modulus for the a-CN_xH films, v_i and v_s are the Possion's ratio of diamond (0.07) and the a-CN_xH films (0.2), E_i and E_s are the Young's modulus of diamond (1,141 GPa) and the deposited films. The inset in Fig. 3 demonstrates the variations of the hardness and the Young's modulus of the films with the working pressure. It can be observed that the hardness and the Young's modulus of the films decreased with increasing working pressure. The maximum hardness and Young's modulus of 20.0 GPa and 160 GPa was obtained for the film grown at 5.0 Pa.

The elastic recovery of the films were calculated from the load-displacement curves as shown in Fig. 3, using $R = (h_{max} - h_{res}) \times 100$ [29, 30]. The R was found approximately 82% at the peak load of 0.6 mN for the film deposited at 5.0 Pa. The R of the films prepared at different deposition pressures are listed in Table 2. It can be found that the R reduced from 82% to 71% with increasing deposition pressure, which accounts for that the degenerated elastic properties of the a-CN_xH films.

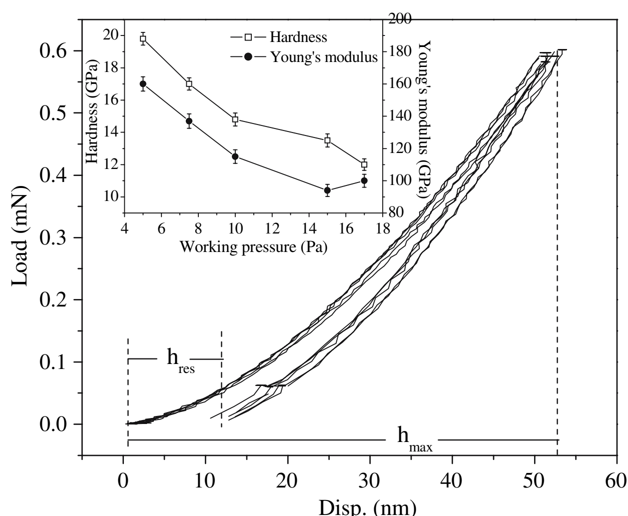

Fig. 3 Load-displacement curves for the a-CN_xH film deposited at 5.0 Pa and the variation of Young's modulus with deposition pressure

Adhesion of films

Figure 4 shows the adhesion strength of the films deposited at different working pressure by WS-92 scratch tester. The scratch process is monitored using an acoustic emission (AE). It is seen that the scratch process of the deposited films could be divided into three stages. In the initial scratch stage, because the load is small and the diamond tip performed the scratch in the films, the AE signal is stable and almost near nought. With the load increasing constantly, the weak and transitory AE appeared in the second scratch stage, which indicates that the micro-crack occurred and the film starts to peel off as the small fragments. In the third scratch stage, the AE signal sharply increased at a certain load and this load was defined as the critical load (L_c) and used as a quasi-quantitative criterion to evaluate the adhesion strength of the a-CN_xH films. Then the AE signal became violent and continuous with the increase of load above the critical load, which indicates that the diamond indenter reaches and contacts with the substrate at this point or later, and the a-CN_xH films underwent failure at this stage.

Figure 5 gives the SEM pictures of the scratched tracks at the above-mentioned three stages, taking example for the film deposited at 5.0 Pa. Mild plastic deformation and adhesion signs are visible along the scratch track edges as

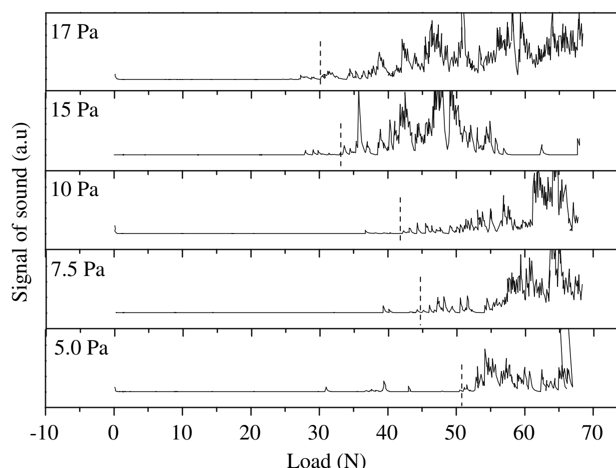

Fig. 4 Scratch test data for the a-CN_xH film deposited at different working pressure

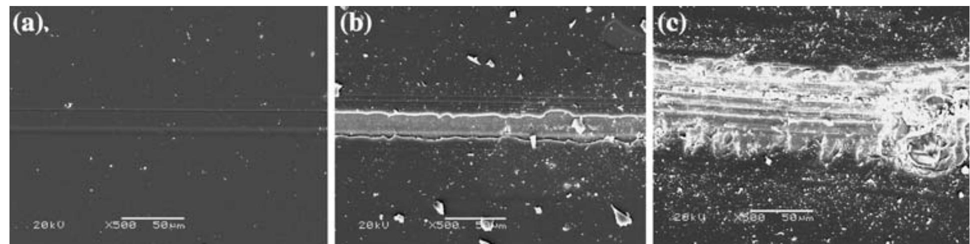

Fig. 5 SEM micrographs of the scratched tracks of a-CN_xH film deposited at 5.0 Pa in (**a**) initial stage, (**b**) intermediate stage, and (**c**) final stage

for the first scratching stage when the load is small (see Fig. 5a). The plastic deformation and adhesion become more severe as the normal force close to the critical load (52.0 N), at this stage the a-CN_xH film with low fracture toughness experiences brittle fracturing and local micro-crack failure (see Fig. 5b). When the normal load exceeds 52.0 N, a large portion of the film is peeled off and the scratched track shows signs of catastrophic plastic deformation and large extent of adhesion (see Fig. 5c), which corresponds to the complete failure of film.

The scratch processes of other films deposited at different pressures are also analogous and the critical loads are listed in Table 2. It can be observed that the critical load of the film grown at 5.0 Pa is highest, indicating a good adhesion between the film and the substrate. The critical loads of the a-CN_xH films decreased rapidly from 52.0 N to 30.0 N with the increase of the pressure from 5.0 Pa to 17.0 Pa. The poor adhesion of the a-CN_xH films deposited at a high working pressure could be partly ascribed to the obvious increase in the surface roughness. In addition, the adhesion of the films depends not only on the mechanical strength (adhesion, cohesion) of the film-substrate system, but also on the film hardness and the N content inside the films [31, 32]. The N content in films increased clearly with the increase of the deposition pressure, excess N content led to the structural transformation from sp^3 to sp^2-like carbon–nitrogen network in the films, and the film hardness was weakened, which led to the decrease of the film adhesion strength. Indeed, the scratch process of soft film is shorter than that of the harder film. Therefore, an obvious decrease in critical load is observed at higher working pressure.

Friction and wear behavior

Figure 6 shows the variation of the friction coefficient of the films deposited at different pressure against a Si_3N_4 ball at a load of 1.0 N. In all the samples, it was found that the friction coefficient is characterized by three stages: an initial stage of high friction followed by a second steady state stage of reduced friction coefficient, and then a third film failure stage characterized by sharp increase of friction coefficient. Broitman et al. [33] thought that in the initial stage, the friction coefficient is controlled by film roughness and the formation of a transfer layer (tribo-layer), and in the second stage the friction coefficient and wear are controlled by the nature of the film. Sánchez-López et al. [34] also reported that the higher friction coefficient in the initial stage probably corresponded to the removal of the oxidized top layers, polishing of microasperities, and build up of the transfer film. In the third stage, the friction coefficient reached the values as high as 0.5–0.6, which indicates the complete degradation of the film. The sliding time at this point was defined as the wear life of the films.

The variation of the wear life for the films prepared at different working pressure was shown in Fig. 7. It can be seen that the wear life of the deposited films sharply increased with the increase of the working pressure from 5.0 Pa to 7.5 Pa, a further increase in the deposition pressure led to a decrease in the wear life, and the a-CN_xH film deposited at 7.5 Pa had the largest wear life as much as 2,390 s, but the film deposited at 17.0 Pa showed the worst wear durability about only 665 s. Low hardness, high roughness and poor adhesion of this film would be the main reasons for its worst wear durability. Moreover, the a-CN_xH films prepared at different working pressures had similar average friction coefficients within the range of 0.18–0.20 (see Table 2). In other words, the deposition pressure seemed to have slight effect on the average friction coefficients, whereas the surface roughness and adhesion strength gradually deteriorated with the increase of deposition pressure. The variations in the structure and mechanical properties of the films with increasing working pressure, which are shown in Figs. 1–6, may play important role in controlling the friction behavior of films.

Conclusions

It is feasible to prepare a-CN_xH films on single crystal silicon wafer using DC-RF-PECVD at working pressure of 5.0–17.0 Pa. The surface morphology, elastic, adhesion and tribological properties of the films were strongly dependent on the deposition pressure. With increasing pressure from 5.0 Pa to 17.0 Pa, the I_D/I_G ratio increases from 0.85 to 1.87 and the roughness values of the films increased from 0.18 nm to 0.50 nm, while the critical load

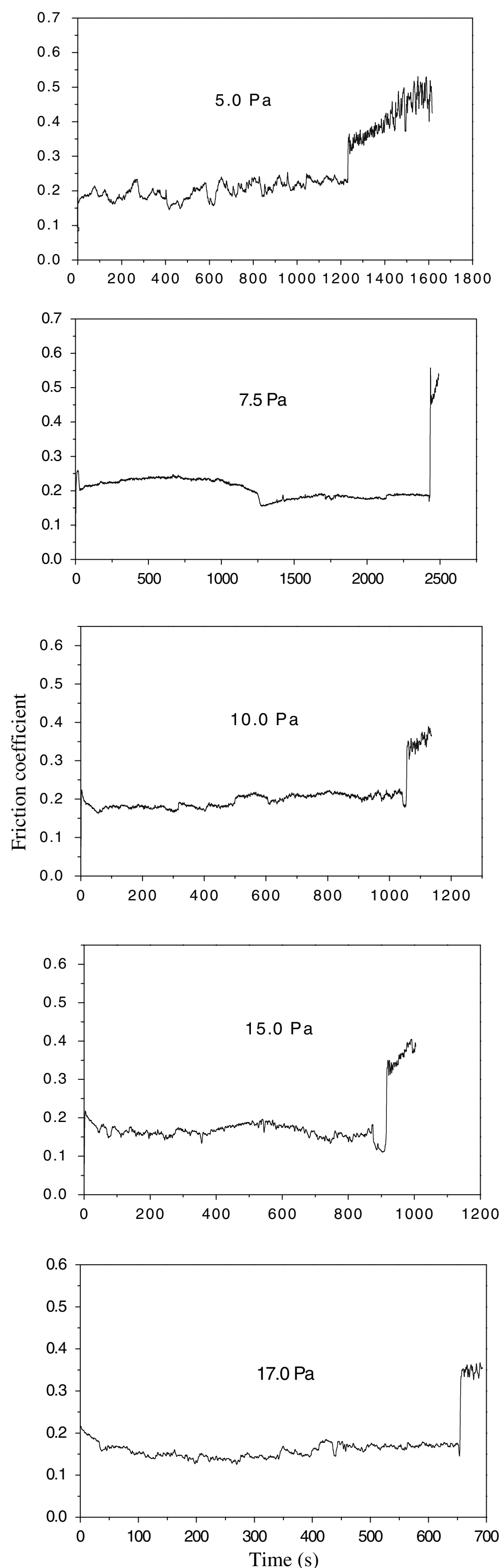

◀ **Fig. 6** Variation of the friction coefficient with sliding time for the a-CN_xH films deposited at various working pressure and tested against a Si_3N_4 ball at a load of 1.0 N

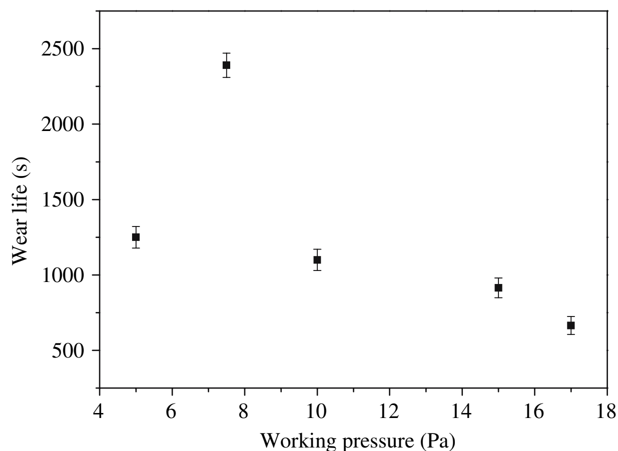

Fig. 7 Wear life of the a-CN_xH films as a function of working pressure

decreased from 52.0 N to 30.0 N, and the Young's modulus and elastic recovery of the films decreased from 160 GPa and 82% to 94.0 GPa and 71%. Moreover, the wear life of the a-CN_xH films sharply improved as the working pressure increased from 5.0 Pa to 7.5 Pa, then it dramatically decreased with further increase in the deposition pressure from 7.5 Pa to 17.0 Pa, as a result the film deposited at 7.5 Pa exhibited the largest wear life as much as 2,390 s. Although, the a-CN_xH films prepared at different pressures had similar average friction coefficients in the range of 0.18–0.20, the surface roughness and adhesion strength gradually deteriorated with increasing deposition pressure.

Acknowledgements The authors are grateful to the National Natural Science Foundation of China (Grant No. 50405040 and No. 50432020), "973" program of China (Grant No. 2007CB607601), and the Innovative Group Foundation from NSFC (Grant No. 50421502) for financial support.

References

1. Liu AY, Cohen ML (1989) Science 245:841
2. Liu AY, Cohen ML (1990) Phys Rev B 41:10727
3. Liu AY, Wentzcovitch RM (1994) Phys Rev B 50:10362
4. Jiang LD, Fitzgerald AG, Rose MJ (2000) Appl Surf Sci 158:340
5. Fernandez A, Ternandez-Ramos C, Sanchez-Lopez JC (2003) Surf Coat Technol 163–164:527
6. López S, Dunlop HM, Benmalek M, Tourillon G, Wong M-S, Sproul WD (1997) Surf Interface Anal 25:315

7. Okada T, Yamada S, Takeuchi Y, Wada T (1995) J Appl Phys 78:7416
8. Ogata K, Chubaci JFD, Fujimoto F (1994) J Appl Phys 76:3791
9. Meskinis S, Andrulevicius M, Kopustinskas V, Tamulevicius S (2005) Appl Surf Sci 249:295
10. Boyd KJ, Marton D, Todorov SS, Al-Bayati AH, Kulik J, Zuhr RA, Rabdais JW (1995) J Vac Sci Technol A 13:2110
11. Bhattacharyya S, Vallee C, Cardinaud C (1999) J Appl Phys 85:2162
12. Égerházi L, Geretovszky Zs, Szörényi T (2005) Appl Surf Sci 247:182
13. Szörényi T, Fogarassy E (2003) Appl Surf Sci 208–209:502
14. Rusop M, Omer AMM, Adhikari S, Adhikary S, Uchida H, Soga T, Jimbo T, Umeno M (2005) Diam Relat Mater 14:975
15. Motta EF, Pereyra I (2004) J Non-Cryst Solids 338–340:525
16. Uddin MN, Fouad OA, Yamazato M, Nagano M (2005) Appl Surf Sci 240:120
17. Durand-Drouhin O, Benlahsen M, Clin M, Zellama K (2004) Diam Relat Mater 13:1854
18. Cheng YH, Sun ZH, Tay BK, Lau SP, Qiao XL, Chen JG, Wu YP, Xie CS, Wang YQ, Xu DS, Mo SB, Sun YB (2001) Appl Surf Sci 182:33
19. Takadoum J, Rauch JY, Cattenot JM, Martin N (2003) Surf Coat Technol 174–175:427
20. Li HX, Xu T, Chen JM, Zhou HD, Liu HW (2003) J Phys D: Appl Phys 36:3183
21. Hao JY, Xu T, Liu WM (2005) J Non-Cryst Solids 351:3671
22. Hao JY, Xu T, Liu WM (2005) Mater Sci Eng A 408:297
23. Schwan J, Ulrich S, Batori V, Ehrhardt H, Silva SRP (1996) J Appl Phys 80:440
24. Ferrari AC, Robertson J (2000) Phys Rev B 61:14095
25. Ferrari AC, Rodil SE, Robertson J (2003) Phys Rev B 67:155306
26. Shiao J, Hoffman RW (1996) Thin Solid Films 283:145
27. Bhattacharyya S, Cardinard C, Turban G (1998) J Appl Phys 83:4491
28. Sheeja D, Tay BK, Lau SP, Shi X (2001) Wear 249:433
29. Chowdhury S, Laugier MT, Rahman IZ (2004) Diam Relat Mater 13:1543
30. Pharr GM (1998) Mater Sci Eng A 253:151
31. Chowdhury AKMS, Cameron DC, Hashmi MSJ (1999) Surf Coat Technol 116–119:46
32. Wu W, Hon M (1999) Thin Solid Films 345:200
33. Broitman E, Hellgren N, Wänstrand O, Johansson MP, Berlind T, Sjöström H, Sundgren JE, Larsson M, Hultman L (2001) Wear 248:55
34. Sánchez-López JC, Belin M, Donnet C, Quirós C, Elizalde E (2002) Surf Coat Technol 160:138